environmental microbiology

Environmental Microbiology (2018) **20**(10), 3811–3824 doi:10.1111/1462-2920.14396

Pigmented microbial eukaryotes fuel the deep sea carbon pool in the tropical Western Pacific Ocean

Dapeng Xu ,[1]* Ping Sun,[2] Yizhe Zhang,[1] Ran Li,[1] Bangqin Huang,[2] Nianzhi Jiao,[1] Alan Warren[3] and Lei Wang[2]

[1]*State Key Laboratory of Marine Environmental Science, Institute of Marine Microbes and Ecospheres, College of Ocean and Earth Sciences, Xiamen University, Xiamen, 361102, China.*

[2]*Key Laboratory of the Ministry of Education for Coastal and Wetland Ecosystem, College of the Environment and Ecology, Xiamen University, Xiamen, 361102, China.*

[3]*Department of Life Sciences, Natural History Museum, London, SW7 5BD, UK.*

Summary

Phototrophic microbial eukaryotes dominate primary production over large oceanic regions. Due to their small sizes and slow sinking rates, it is assumed they contribute relatively little to the downward export of organic carbon via the biological pump. Therefore, the community structure of phototrophic cells in the deep ocean has long been overlooked and remains largely unknown. In this study, we used an integrative approach, including epifluorescence microscopy, sequencing of 18S rRNA and photosystem-II psbA gene transcripts, to investigate phototrophic microbial eukaryotes in samples collected from the tropical Western Pacific Ocean. It was found that: (i) pigmented nano-sized eukaryotes (PNEs) are ubiquitous in the deep Western Pacific Ocean down to 5000 m depth; (ii) the PNE community is dominated by cells 2–5 μm in size; (iii) their abundance is significant, averaging 4 ± 1 (± s.e.) cells ml^{-1} in waters below 1000 m which is comparable to that of heterotrophic nanoflagellates; (iv) the active pigmented microbial eukaryotes in the deep waters are highly diverse and dominated by Haptophyta followed by Chlorophyta and Bacillariophyta; (v) PNEs in deep waters were likely transported from surface ocean by various fast-sinking mechanisms, thus contributing to the biological pump and fuelling the deep-sea communities by supplying fresh organic carbon.

Received 29 September, 2017; revised 24 August, 2018; accepted 25 August, 2018. *For correspondence.E-mail dapengxu@xmu.edu.cn; Tel. +86 592 288 0842; Fax +86 592 288 0150.

Introduction

Marine phytoplankton encompasses prokaryotic and eukaryotic organisms that are capable of oxygenic photosynthesis and inhabit the photic zone of all oceans (Falkowski *et al*., 2004; Worden *et al*., 2004). They account for almost half of all photosynthetic activity on Earth and thus play a fundamental role in marine ecosystems and global biogeochemical processes. In vast areas of the oceans, especially the oligotrophic regions, the majority of primary production is performed by small-sized cells, that is, the picoplankton (< 2–3 μm in diameter) and nanoplankton (2–20 μm in diameter) (Marañón *et al*., 2001). Among these minute cells, the abundance of phototrophic microbial eukaryotes is two to three orders of magnitude lower than their prokaryote counterparts, the cyanobacteria. However, because of their equivalent or higher growth rates and relatively larger cell size, they can dominate carbon biomass and net production both in coastal waters (Massana *et al*., 2004a; Worden *et al*., 2004) and in the open ocean (Li, 1995; Not *et al*., 2008; Jardillier *et al*., 2010). In addition, compared with cyanobacteria that are dominated by just two genera (*Prochlorococcus* and *Synechococcus*), photosynthetic microbial eukaryotes are much more diverse and include representatives of almost all major clades of the eukaryotic phylogenetic tree (Massana, 2011; Decelle *et al*., 2015).

The biological pump involves a series of processes through which CO_2 is fixed as organic matter by photosynthesis and then transferred to the deep ocean, resulting in the temporary or permanent storage of carbon (Sigman and Haug, 2006). Traditionally, large and 'heavy' phytoplankton cells such as diatoms are thought to be the main contributors to the downward transportation of organic carbon through the biological pump. The pico/nano-sized phototrophic eukaryotes are generally believed to contribute relatively little to carbon export due to their smaller sizes, slow sinking rates and rapid utilization in the microbial loop in the photic zone. It has been argued, however, that the contribution of picoplankton to

carbon export from the photic zone is proportional to their total net primary production, which is significant considering their high abundances and production rates (Richardson and Jackson, 2007).

Early studies reported the occasional presence of well-preserved phytoplankton cells in the deep-sea samples, although these observations were considered anecdotal and have long been overlooked (Kimball *et al*., 1963; Smayda, 1971; Wiebe *et al*., 1974). More recently, however, intact, viable diatom cells have been reported from deep-sea sediment traps and downward export pulse has been observed at Station ALOHA (Scharek *et al*., 1999; Karl *et al*., 2012). Furthermore, a global survey employing DNA sequencing has also suggested the presence of phototrophic signals in the deep ocean (Pernice *et al*., 2015b). The ubiquitous presence of healthy photosynthetic cells (mainly diatoms) and 16S rRNA gene sequences of photosynthetic cells (cyanobacteria and algal chloroplasts) at depths of up to 4000 m in the dark ocean on a global scale has been reported (Agusti *et al*., 2015). Finally, based on the sequencing both of the 18S rRNA and its gene, active phototrophic microbial eukaryotes were confirmed to be present in the deep waters of the South China Sea (Xu *et al*., 2017b). Although these pioneering studies have revealed the presence of phototrophic microbial eukaryotes in deep oceans, knowledge of their source, community structure, biogeography and function remain largely unknown.

In the present study, an integrative approach including fluorescence microscopy, high-throughput sequencing (HTS) of the hyper-variable V9 region of 18S rRNA and cloning and sequencing of photosystem-II psbA gene transcripts, was used to explore the abundance (nano-sized only), size fractions (2–5 μm, 5–10 μm and 10–20 μm) and phylogenetic identity (evidence from both 18S rRNA and photosystem-II psbA gene transcripts), of phototrophic microbial eukaryotes in the deep tropical Western Pacific Ocean. In so doing, the community structure of phototrophic microbial eukaryotes in deep oceanic waters is revealed for the first time, confirming their contributions to the downward transportation of organic carbon through the biological pump. The potential presence of mixotrophic microbial eukaryotes in the deep tropical Western Pacific Ocean is also revealed.

Results

Distribution of environmental variables

In total, 110 water layers from 11 stations in the tropical Western Pacific Ocean were sampled (Fig. 1). The water temperature, salinity and chlorophyll *a* (Chl *a*) at each depth interval are summarized in Supporting Information Fig. S1. A well-defined pycnocline was found with the steepest gradients in salinity (27.0–35.3) and temperature (30.5°C–1.6°C) between 20 and 100 m (Supporting Information Fig. S1A and B). Surface (5 m) Chl *a* concentration was low (0.02–0.16 μg L^{-1}) throughout the study area reflecting the oligotrophic conditions in the tropical Western Pacific Ocean. The deep chlorophyll *a* maximum (DCM) layer was found at 50 m at P14, 75 m at P12 and 100 m at the rest of sampling stations (Supporting Information Fig. S1C). Phytoplankton pigments measured at 5 m, DCM and 200 m of all sampling stations revealed that the contribution of eukaryotes to total Chl *a* was 9%–19% (on average 13%), 9%–50% (on average 32%) and 10%–100% (on average 43%) respectively (data not shown). Using CHEMTAX, the relative contributions of six major eukaryotic chemotaxonomic groups, that is, haptophytes, prasinophytes, cryptophytes, chlorophytes, diatoms and dinoflagellates, to total eukaryotic Chl *a* were determined. At all depths of all sampling stations, haptophytes were clearly the dominant pigmented group among eukaryotes, their relative contributions to total eukaryotic Chl *a* being 57%–74% (on average 64%) at 5 m, 58%–94% (on average 77%) at DCM and 0%–92% (on average 67%) at 200 m. Excluding P14, where no haptophyte pigment signal was recovered at 200 m, the contribution of haptophytes to total eukaryotic Chl *a* reached 42%–92% (on average 75%) at 200 m (Supporting Information Fig. S2A–C). Generally, haptophytes were the highest contributor to the total eukaryotic Chl *a* at DCM, with a lower relative contribution at 200 m and lower still at 5 m. The absolute Chl *a* concentration of haptophytes ranged 5.9–32.2 ng l^{-1} (on average 14.1 ng l^{-1}) at 5 m, 20.6–170.9 ng l^{-1} (on average 118.1 ng l^{-1}) at DCM and 0–16.2 ng l^{-1} (on average 2.7 ng l^{-1}) at 200 m respectively (Supporting Information Fig. S2D).

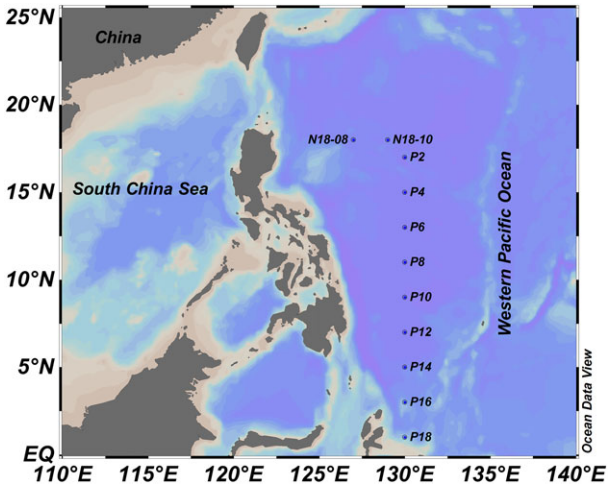

Fig. 1. Geographic locations of the sampling stations. The map was generated using Ocean Data View 4 software (Schlitzer, 2010). [Color figure can be viewed at wileyonlinelibrary.com]

The abundances of bacteria and archaea decreased with increasing water depth, from 1.3–8.5 $\times$ 10^5 cells ml^{-1} in the euphotic zone to 1.3–3.5 $\times$ 10^4 cells ml^{-1} in the bathypelagic zone (Supporting Information Fig. S3A). The abundances of *Prochlorococcus* ranged from 1.8 $\times$ 10^2 to 2.6 $\times$ 10^5 cells ml^{-1} in the euphotic zone with highest abundances generally occurring at the DCM (Supporting Information Fig. S3B). The abundances of *Synechococcus* were about one order of magnitude lower than those of *Prochlorococcus*, ranging from 1.5 $\times$ 10^2 to 4.9 $\times$ 10^4 cells ml^{-1} (Supporting Information Fig. S3C). Pigmented picoeukaryote abundances ranged from 20 to 5.2 $\times$ 10^3 cells ml^{-1} (Supporting Information Fig. S3D).

Enumeration of pigmented nano-sized eukaryotes by microscopy

Fluorescence microscopy examinations of pigmented nano-sized eukaryotes (PNEs) (2–20 μm) were performed for all 110 samples collected (Supporting Information Fig. S4). This showed not only the vertical distribution pattern of abundance but also the cell-size structure of PNEs in water columns of the Western Pacific Ocean. Interestingly, PNEs were found not only in all 66 euphotic zone samples (5–200 m) where photosynthesis could be achieved but also in all 11 mesopelagic zone samples (200–500 m) and 61% of the 33 deep-sea (≥ 1000 m) samples including the greatest depth sampled (5000 m at P12). The abundance of PNEs varied among the three depth zones with the highest abundance generally occurring in the DCM (Fig. 2). In the waters at 5–50 m, the average (± s.e.) abundance of PNEs was 768 ± 59 cells ml^{-1}. At 75–100 m, their abundance averaged 672 ± 64 cells ml^{-1}. At 200–500 m, their abundance dropped to 31 ± 10 cells $ml^{-1}$and at 1000–3000 m their abundance averaged 4 ± 1 cells ml^{-1} (Table 1). Generally, the abundance and biomass of PNEs did not change much in waters ≤ 100 m but decreased sharply from 100 to 200 m and maintained low abundance in waters > 200 m (Fig. 3A and B). In general, the abundance of PNEs decreased with depth with log–log regression slopes (Fig. 3C) and declined more steeply than that of bacteria and archaea (Fig. 3D). Additionally, epifluorescence microscopy observation allowed an approximate estimate of the size structure of the PNE community. The PNE communities (both abundance and biomass) were dominated by cells in the size range 2–5 μm at all depths followed by cells in the size range 5–10 μm. In waters below 200 m, no PNEs larger than 5 μm were found. PNEs with size range 10–20 μm were only found in certain samples at 5 m (Fig. 3A and B).

Active microbial eukaryote communities revealed by high-throughput sequencing of V9 regions of 18S rRNA

Following high-throughput sequencing of V9 regions of the reverse-transcribed 18S rRNA and the removal of low quality reads, potential chimeras, reads that were not assigned as eukaryotes and singletons, there were 371 834 reads representing both protistan and metazoan taxa, ranging 25 388–48 813 reads per sample. Reads affiliated with Metazoa were removed from the dataset resulting in 7708–40 497 reads per sample (Supporting Information Table S1). Notably, a large portion (81.8%) of the reads from the deepest sample (5000 m) collected at station P12 (P12.5K) was affiliated with Cnidaria (data not shown). To normalize sampling effort, OTU counts

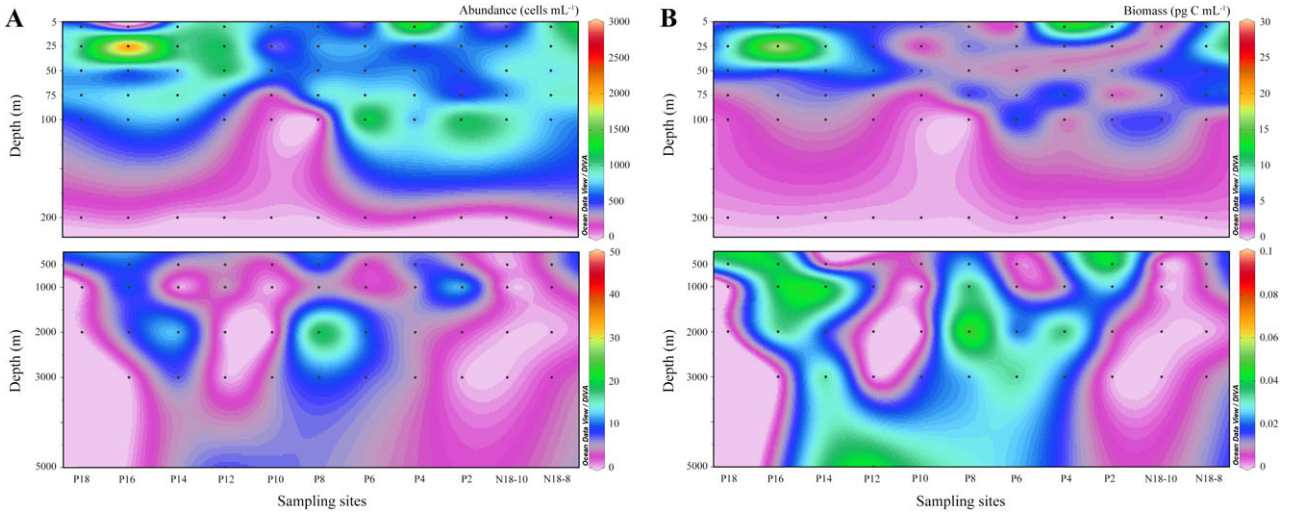

Fig. 2. Abundance (A) and biomass (B) of pigmented nano-sized eukaryotes (PNEs) in the water columns of the Western Pacific Ocean. The map was generated using Ocean Data View software (Schlitzer, 2010). [Color figure can be viewed at wileyonlinelibrary.com]

Table 1. Abundance and biomass of PNEs in the tropical Western Pacific Ocean

	Average ± SE	
Depth (m)	Abundance (cells ml^{-1})	Biomass (pg C ml^{-1})
5–50	768 ± 59	5360 ± 567
75–100	672 ± 64	3013 ± 339
200–500	31 ± 10	88 ± 29
1000–3000[a]	4 ± 1	16 ± 3

[a]. Including one sample collected at 5000 m depth.

were rarefied at a uniform sequencing depth based on the lowest sequence count affiliated with microbial eukaryotes (7708 reads) of sample P12.5K.

Nonmetric multidimensional scaling ordination (nMDS) analysis showed that all samples were clustered into two groups according to the depth where samples were collected, one containing samples from the euphotic zone (25 and 75 m) and the other containing samples from deep waters (≥ 500 m) (Fig. 4A). Statistical analyses showed the composition of the two groups differed significantly from one another (ANOSIM, R = 0.7255, p = 0.0032). This grouping pattern was also supported by principle component analysis (PCoA) of community taxonomic relatedness quantified by the Unweighted Unifrac metric which compares samples based on the phylogenetic relatedness of OTUs in a community without taking into account relative OTU abundance (Fig. 4B). Therefore, the community composition is described below according to this vertical distribution pattern. At the supergroup level, the active microbial eukaryote communities in the euphotic zone were characterized by high relative sequence abundances of Stramenopiles (on average 48%), followed by Alveolata (on average 25%) and Hacrobia (on average 16%) (Supporting Information Fig. S5A). The other supergroups, that is, Amoebozoa,

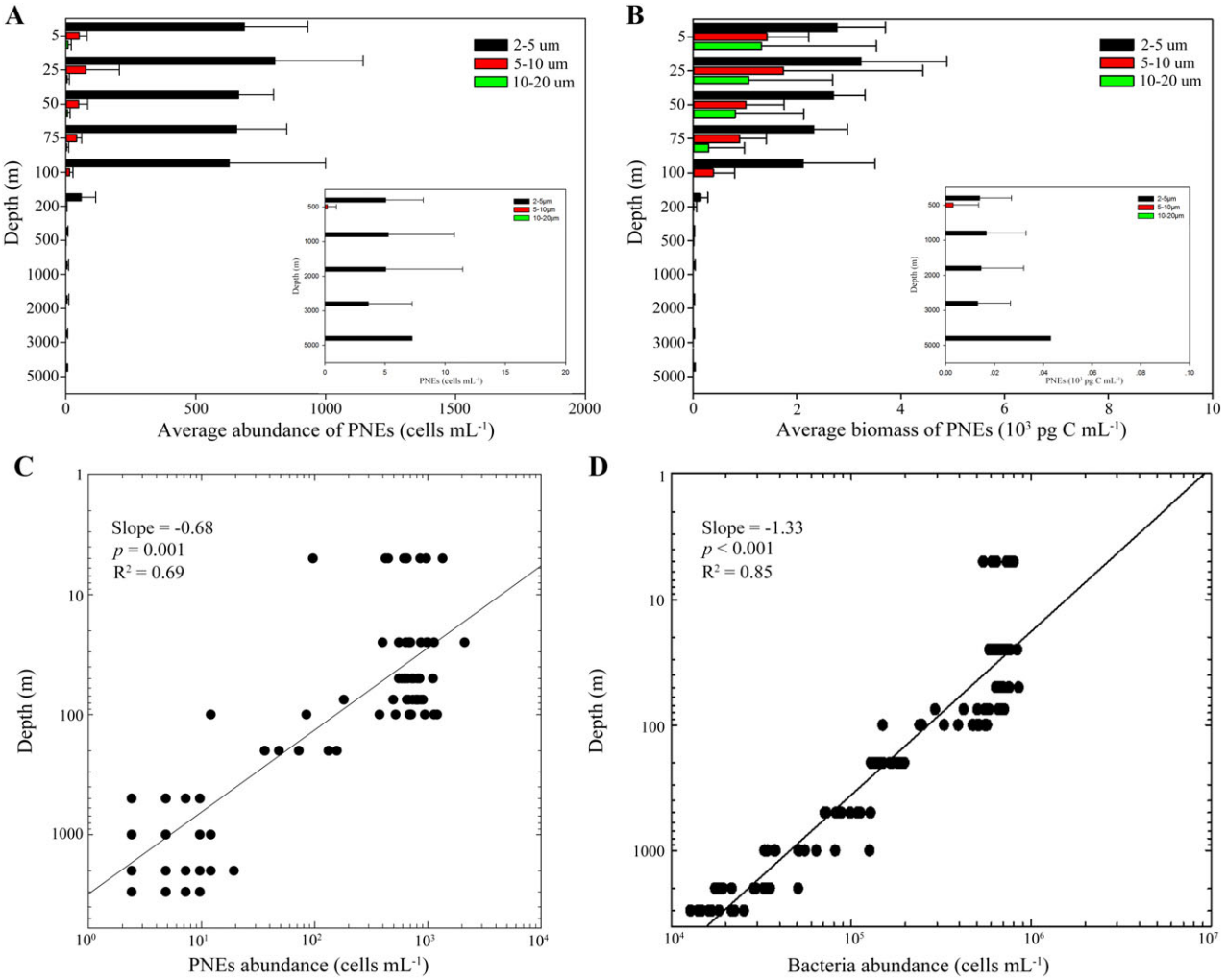

Fig. 3. Size-fractionated abundance (A) and biomass (B) distribution of PNEs in the water column of the Western Pacific Ocean. Depth profiles of PNEs (C) and bacteria/archaea abundance (D). [Color figure can be viewed at wileyonlinelibrary.com]

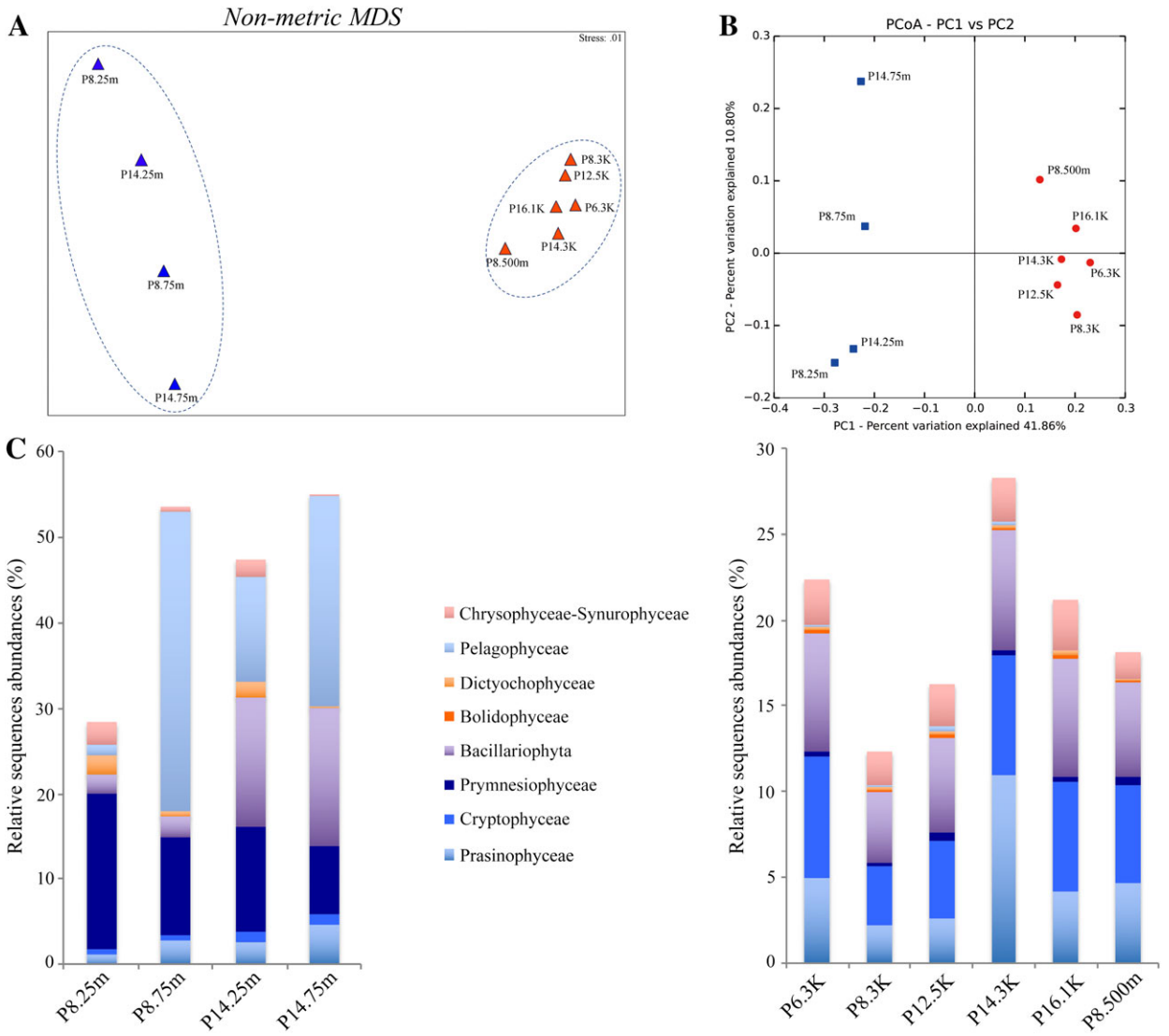

Fig. 4. Plots of nonmetric multidimensional scaling (nMDS) ordination (A) and unweighted UniFrac principal coordinates analysis (PCoA) (B) of microbial eukaryotes based on community distance matrices inferred from V9 regions of 18S rRNA sequencing. Relative 18S rRNA sequence abundance of major phototrophic microbial eukaryotes in euphotic and deep-sea zones (C). [Color figure can be viewed at wileyonlinelibrary.com]

Apusozoa, Archaeplastida, Excavata, Opisthokonta, Picozoa and Rhizaria, were only minor contributors to the microbial eukaryotic communities. By contrast, the most dominant supergroup in the deep-sea samples (500–5000 m) was Alveolata (on average 51%), followed by Stramenopiles (on average 19%), Hacrobia (on average 6%), Rhizaria (on average 8%) and Opisthokonta (on average 8%) (Supporting Information Fig. S5A). The third most dominant supergroup was not always consistent, however, but shifted between Rhizaria and Hacrobia in different samples (Supporting Information Fig. S6). In terms of OTU richness at the supergroup level, the contributions of Stramenopiles and Alveolata were almost equal both in the euphotic zone (on average 31.4% and 30.5% respectively) and in the deep-sea (on average 27.6% and 28.5%, respectively), while that of Hacrobia (on average 13.5% and 10.5%, respectively) and Rhizaria (on average 10.9% and 13.8%, respectively) varied in the two groups relative to each other (Supporting Information Fig. S5B).

In common with the results from epifluorescence microscopy examination, HTS also recovered possible phototrophic signals in all deep-sea samples. For the comparison of phototrophic signals from shallow and deep waters, only major phototrophic groups, that is, Chrysophyceae–Synurophyceae, Pelagophyceae, Dictyochophyceae, Bolidophyceae, Bacillariophyta, Haptophyta (mainly Prymnesiophyceae), Cryptophyceae and Prasinophyceae, were considered in the present analysis. The contributions of major phototrophic groups to

total microbial eukaryote communities in the shallow waters ranged 28%–55%, which is higher than those in the deep-sea which ranged from 18% to 28% (Fig. 4C). Even in the sample from the greatest depth (5000 m: P12.5K), the contribution of phototrophic signal to the total eukaryotic community still reached 16.3%. In the shallow waters, the three most dominant phototrophic groups were Prymnesiophyceae, Pelagophyceae and Bacillariophyta, the contributions of which differed in different samples (Fig. 4C). In deep-sea samples, phototrophic groups were dominated by Bacillariophyta, Cryptophyceae and Prasinophyceae with their contributions to total microbial eukaryote communities differing among samples (Fig. 4C). In terms of the entire microbial eukaryote communities, phototrophic groups ranked among the top 10 dominant groups in most deep-sea samples (Supporting Information Fig. S7).

Phototrophic microbial eukaryotes revealed by sequencing of psbA gene transcripts

To avoid the masking of heterotrophic microorganisms resulting from rRNA sequencing, the functional protein-coding gene for D1 of photosystem-II reaction centre (psbA) was cloned and sequenced to reveal the active phototrophic microbial eukaryotes in the water column. After removing potential chimeras and sequences of bacteria/archaea and virus/phage origin, 617 sequences (~ 750 bp) affiliated with microbial eukaryotes (Dinophyceae, Cryptophyta, Euglenozoa, Haptophyta, Cercozoa, Bacillariophyta, Chrysophyceae, Dictyochophyceae, Pelagophyceae, Pinguiophyceae and Chlorophyta) remained. Because of the lack of phenotypic and systematic data on phototrophic microbial eukaryotes in deep oceanic waters, sequences were further assigned taxonomy by blasting against GenBank database to reveal both of their nearest neighbour (NN) and nearest named neighbour (NNN). Generally, as expected, the similarities of the representative sequence to their NN were higher than to their NNN. In some groups, similarities to their NNN were rather low, for example, Chrysophyceae (89.0%–91.6%, on average 90.3%) and Chlorophyta (89.5%–99.6%, on average 91.4%) (Table 2).

For all psbA sequences retrieved, Haptophyta was the dominant group (56.6%), followed by Chlorophyta (15.7%) and Bacillariophyta (13.0%) (Table 2). Among the Haptophyta-affiliated sequences, the NNN of 62.6% was *Emiliania huxleyi* (GenBank accession number JN022705) and of 28% was *Phaeocystis globosa* and *Phaeocystis antarctica* (GenBank accession numbers KC900889 and JN117275, respectively). The rest (10%) belonged to Prymnesiales. For sequences affiliated with Chlorophyta, the NNN of 71% belonged to Prasinophyceae. The third most frequently encountered group was Bacillariophyta, which included 12.6% of all psbA sequences. Bacillariophyceae, Coscinodiscophyceae, Fragilariophyceae and Mediophyceae, accounted for 16.1%, 59.8%, 6.9% and 17.2%, respectively, of all Bacillariophyta-affiliated sequences. The other phototrophic groups, that is, Dinophyceae, Cryptophyta, Euglenozoa, Cercozoa, Chrysophyceae, Dictyochophyceae, Pelagophyceae and Pinguiophyceae, were only minor contributors to the total psbA sequences (Table 2).

Similar to the result of 18S rRNA HTS, sequencing of psbA gene transcripts also revealed the presence of active phototrophic microbial eukaryotes in all deep-sea samples, with their relative sequence abundances differing among sites and depths (Supporting Information Fig. S8). For phototrophic microbial eukaryotes in shallow and deep waters, Haptophyta was the main contributor (56% and 60%, respectively) to both communities. Bacillariophyta and Chlorophyta contributed 15% and 12%, respectively, to the group of shallow water communities and 8% and 16%, respectively, to the group of deep-sea communities (Fig. 5A and B).

To determine the possible origin of deep-sea phototrophic microbial eukaryotes, all psbA OTUs were

Table 2. Taxonomic identifications of the psbA genes retrieved from the Western Pacific Ocean, with their number of clones and average similarity (%-S) with the NN and NNN

Group	Number of clones	Number of OTUs	Average %-S to NN (Median, Min–Max)	Average %-S to NNN (Median, Min–Max)
Dinophyceae	12	6	93.4 (95.0, 85.8–97.2)	93.5 (96.1, 85.3–97.2)
Cryptophyta	1	1	99.7	97.1
Euglenozoa	1	1	77.4	78.0
Haptophyta	349	142	96.6 (97.9, 75.6–99.7)	94.9 (95.7, 78.0–99.5)
Cercozoa	14	4	93.9 (92.9, 92.4–97.2)	94.7 (94.4, 92.6–97.4)
Bacillariophyta	80	44	94.0 (93.9, 89.1–99.8)	95.2 (95.6, 89.4–99.9)
Chrysophyceae	26	13	98.5 (98.8, 96.5–99.6)	90.3 (90.5, 89.0–91.6)
Dictyochophyceae	19	7	94.8 (93.0, 91.6–98.7)	92.0 (91.8, 89.8–93.6)
Pelagophyceae	16	5	98.4 (99.2, 93.4–99.7)	94.6 (92.1, 91.2–99.1)
Pinguiophyceae	2	2	90.8 (90.8, 89.1–92.4)	91.1 (91.1, 90.0–92.2)
Chlorophyta	97	42	93.6 (92.8, 86.3–99.5)	91.4 (89.5, 86.5–99.6)

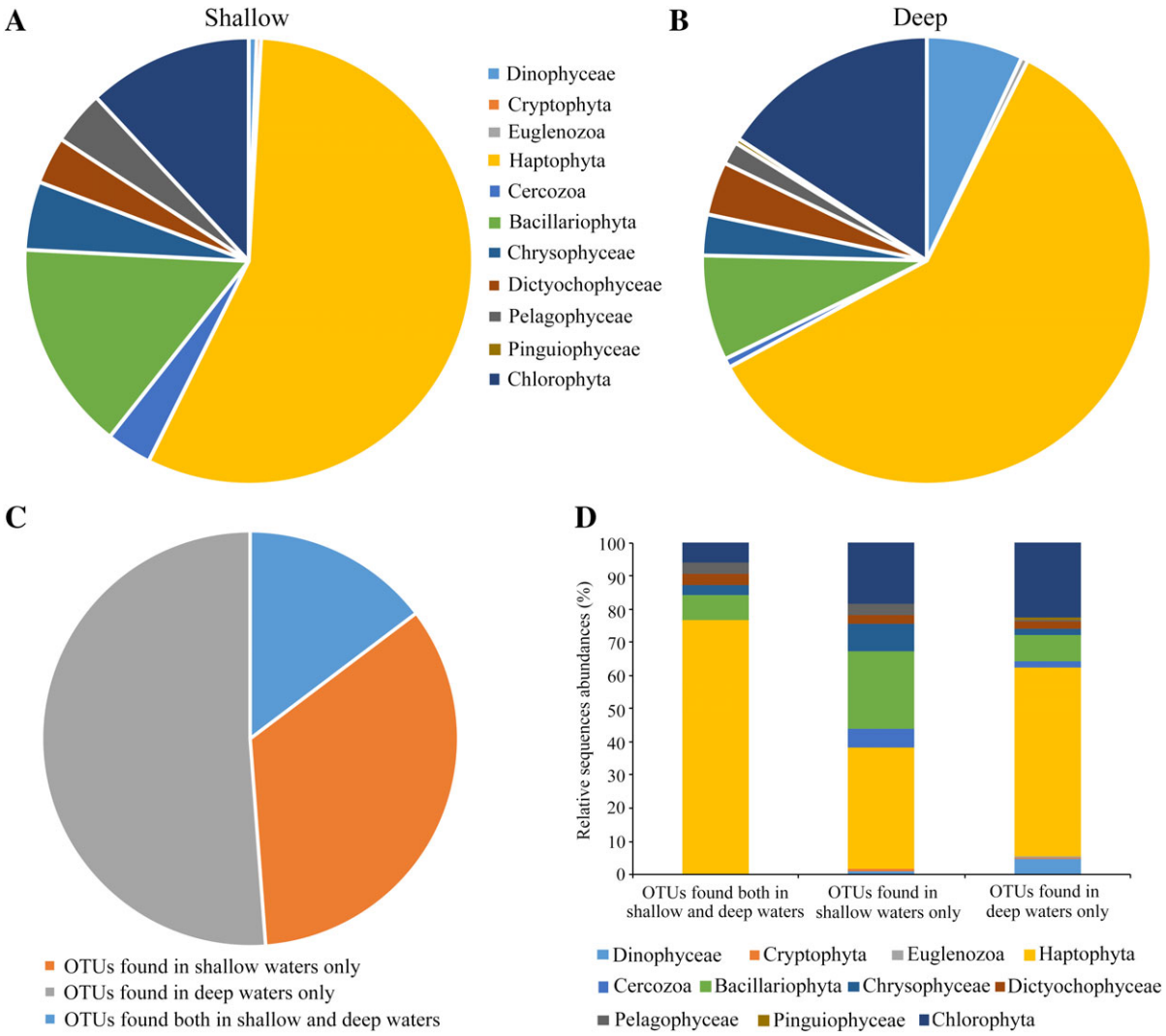

Fig. 5. Taxonomic composition of phototrophic microbial eukaryotes in the shallow (25 and 75 m) (A) and deep (≥ 500 m) (B) waters of the Western Pacific Ocean based on psbA gene transcript sequencing. Proportions of psbA OTUs (C) and community composition (D) of phototrophic microbial eukaryotes among the 'shallow water only' group, the 'deep sea only' group and the 'both shallow and deep sea' group. [Color figure can be viewed at wileyonlinelibrary.com]

clustered into three groups, one containing OTUs occurring in shallow waters only (the 'shallow water only' group), one containing OTUs occurring in deep waters only (the 'deep water only' group) and one containing OTUs occurring in both shallow and deep waters (the 'both shallow and deep waters' group). Fifty-one percent of all phototrophic microbial eukaryote OTUs were found in the 'deep water only' group and 34% were present in the 'shallow water only' group, the remaining 15% occurring in the 'both shallow and deep waters' group (Fig. 5C). In terms of the compositions of these three groups, Haptophyta contributed the most to the three groups (77% of the 'both shallow and deep waters' group, 57% of the 'deep water only' group and 37% of the 'shallow water only' group) (Supporting Information Fig. S8D).

Discussion

Abundance and size fraction distribution of PNEs in the water column of the Western Pacific Ocean

Marine photosynthesis contributes about 50% of total primary production on Earth (Field *et al*., 1998) and that of the phototrophic microbial eukaryotes is agued to surpass other phototrophic organisms in both coastal and oceanic waters (Li, 1995; Worden *et al*., 2004; Li, 2009). Despite their high contributions to the primary production in the surface ocean, the contributions of phototrophic microbial eukaryotes, especially the pico- and nano-sized cells, to the downward transportation of organic carbon through the so-called biological pump has not been appreciated until relatively recently (Bienfang, 1980).

Previous studies on pico-sized phytoplankton showed that these minute cells indeed occurred in both deep oceanic waters and sediments. For example, aggregates of intact *Emiliania huxleyi* and diatom cells were reported from sediment traps (Cadée, 1985; Lampitt *et al*., 1993; Scharek *et al*., 1999) and live *Prochlorococcus* cells were found in mesopelagic waters (Jiao *et al*., 2014). Based on the Malaspina circumnavigation expedition, viable diatoms (mainly micro-sized cells, 20–200 μm) were reported in the deep sea globally (Agusti *et al*., 2015). Richardson and Jackson (2007) proposed that the contribution of picophytoplankton to carbon export is proportional to their total net primary production, which would be extremely high considering they are the main contributors to primary production in the ocean. Compared with pico-sized phytoplankton, however, the contribution of nano-sized (2–20 μm) phototrophic eukaryotes to the downward transportation of organic carbon was largely unknown.

In the present study, pigmented nano-sized eukaryotes (PNEs) collected from 110 samples in the Western Pacific Ocean were examined by fluorescence microscopy. We found that PNEs not only occurred in all 66 samples in the euphotic zone and 11 samples in the twilight zone but were also present in 20 of all 33 deep-sea (≥ 1000 m) samples including one sample from the greatest depth of 5000 m (Fig. 2). Both the abundance and biomass of PNEs were high in the euphotic zone and relatively low in deep waters with a sharp decrease occurring between 100 and 200 m, suggesting the rapid mineralization of PNEs in the euphotic zone (Fig. 3A and B). Previous studies employing microscopy showed large variability of the abundance of deep-sea flagellates (0–20 cells ml^{-1}) in different oceanic regions although without differentiating phototrophs from heterotrophs (see review by Nagata *et al*., 2010). A recent study based on a global expedition which surveyed deep-sea heterotrophic protists (HP) showed that the average abundances of HP ranged from 72 ± 19 cells ml^{-1} in mesopelagic waters down to 11 ± 1 cells ml^{-1} in bathypelagic waters (Pernice *et al*., 2015a). It seems that the abundance of deep-sea PNEs (0–19 cells ml^{-1}) discovered in the present study is slightly lower than, but at the same order of magnitude as, that of the HPs (Pernice *et al*., 2015a). In the present study, the size structure of the PNE community was also investigated which revealed that 2–5 μm cells were the most frequently encountered size-group at all depths, suggesting the considerable contributions of these to the PNE community throughout the water column in tropical oligotrophic oceanic waters.

Phylogenetic identity of phototrophic microbial eukaryotes in deep Western Pacific Ocean

In the present study, both 18S rRNA and psbA gene transcript sequencing were used in order to reveal the active microbial eukaryotes in the deep waters of the Western Pacific Ocean. Signals of phototrophic microbial eukaryotes were found indicating that active phototrophic microbial eukaryotes were widespread in the deep Western Pacific Ocean, the dominant groups being Prasinophyceae, Bacillariophyta and Cryptophyceae as revealed by 18S rRNA sequencing (Fig. 4C). In a recent study, high throughput sequencing of both 18S rRNA and its gene also revealed the presence of active phototrophic microbial eukaryotes in the deep South China Sea. In the same study it was reported that, using RNA/DNA ratio as a proxy, the relative activities of some phototrophic Stramenopiles (e.g., Chrysophyceae, Synurophyceae, Dictyochophyceae and Pelagophyceae) in the deep waters were almost equal with those in the shallow waters (Xu *et al*., 2017b).

In the euphotic zone, 18S rRNA sequencing revealed the dominance of Prymnesiophyceae in P8.25m, Pelagophyceae in P8.75m and P14.75m and Bacillariophyta in P14.25m (Fig. 4C). This finding was not, however, supported by pigment composition analysis which clearly showed that Haptophyta was the dominant phototrophic microbial eukaryote group in the euphotic zone, DCM and 200 m waters (Supporting Information Fig. S2). Previous studies reported that the 18S rRNA gene of haptophytes has a high GC content (57%), which can explain why this group was under-represented in the environmental survey by PCR amplification using eukaryote universal 18S rRNA primers (Moon-van der Staay *et al*., 2001; Massana *et al*., 2004b; Liu *et al*., 2009). In the present study, direct sequencing of 18S rRNA confirmed the presence of active phototrophic microbial eukaryotes in the deep sea but failed to reflect their relative abundances.

Previous studies have found that sequencing of the rRNA gene results in a bias in favour of heterotrophic over phototrophic microorganisms (Vaulot *et al*., 2002). To remediate this effect, psbA, which codes the photosystem II core protein D1, has been recommended as a good marker for a variety of phototrophic marine microbes including picoeukaryotes and cyanobacteria (Zeidner *et al*., 2003; Zeidner and Béjà, 2004; Man-Aharonovich *et al*., 2010). In the present study, both pigment analysis and psbA transcript sequencing showed that the phototrophic microbial eukaryote community was dominated by Haptophyta in the euphotic zone (Fig. 5A). Indeed, previous studies have shown the pervasive presence of pigment 19′-hexanoylfucoxanthin (an accessory photosynthetic pigment found exclusively in chloroplasts of haptophyte origin) in the photic zone of the world's oceans (Lovejoy *et al*., 2006; Not *et al*., 2008; Liu *et al*., 2009) and the dominance of Haptophyta-affiliated psbA transcripts in surface and DCM of the eastern Mediterranean Sea (Man-Aharonovich *et al*., 2010).

The active deep-sea phototrophic microbial eukaryotes in the Western Pacific Ocean included members from Haptophyta, Bacillariophyta, Chlorophyta and other 'common' groups normally encountered in oceanic surface waters. This is consistent with observations by epifluorescence microscopy which revealed PNEs with a variety of different cell shapes in deep-sea waters (Supporting Information Fig. S4), confirming their high diversity in the deep Western Pacific Ocean. To the best of our knowledge, this is the first use of a functional gene to infer deep-sea phototrophic microbial community structure. Analyses of selected deep-water samples revealed that Haptophyta was the major component (comprising 28%–80% of total phototrophic microbial eukaryotes) of deep-sea phototrophic microbial eukaryote communities (Supporting Information Fig. S8). Further analyses showed that the nearest named neighbour (NNN) for most (62.6%) Haptophyta-affiliated sequences was *Emiliania huxleyi* (GenBank accession number JN022705) with genetic similarities ranging from 91.4% to 99.5% (on average 95.6% and median 95.8%). Owing to the low species number and coverage of psbA sequenced for phototrophic microbial eukaryotes in reference databases, the cutoffs of psbA for differentiating species have not reached a consensus. Consequently, it is premature to conclude whether the *Emiliania huxleyi*-type sequences found in the deep Western Pacific Ocean were *E. huxleyi* or its congeners or even other haptophyte genera.

To examine the possible source of the deep-sea phototrophic microbial eukaryotes, all psbA OTUs were clustered into three groups, that is, 'shallow waters only' group, 'deep waters only' group and 'both shallow and deep waters' group. Notably, 15% of all psbA OTUs recovered belonged to the 'both shallow and deep waters' group, indicating these deep-sea phototrophic microbial eukaryotes may come from the euphotic zone (Fig. 5C). This hypothesis is consistent with observations by epifluorescence microscopy examinations which showed that both the abundance and biomass of PNEs dropped sharply in the depth range 100–200 m indicating that most were utilized in the microbial loop at these depths while the rest escaped mineralization through various fast sinking mechanisms such as forming/attaching to phytodetritus, aggregates and faecal pellets (Komar *et al*., 1981; Simon *et al*., 2002; Ploug *et al*., 2008; Iversen and Ploug, 2010). It is known that mesoscale eddies are present in the northwestern subtropical Pacific Ocean (Yuan *et al*., 2007; Yang *et al*., 2013). Both anticyclonic and cyclonic eddies can induce downwelling transportation of particles from the surface ocean. Thus, active physical transportation may also expedite the downward transportation of surface PNEs to the deep-sea in the present study similar to previous observations of *Prochlorococcus* reported from the deep-sea of a nearby area (Jiao *et al*., 2014). Once the PNEs reached the deep sea, they likely meet one of two fates: either (i) they may sink to the sea floor and become buried in the sediment, thereby contributing to the biological pump, or; (ii) they die and their organic remains are released serving as source of labile dissolved organic matter fuelling deep-sea communities. Thus, phototrophic microbial eukaryotes are probably not only major players in the primary production of the euphotic zone but also contribute to the export of organic carbon from the surface to the deep waters of the ocean. However, as the measurement of sinking rates of phototrophic microbial eukaryotes was outside the scope of the present study, this process needs further exploration in order to fully appreciate their contribution to the downward transportation of organic matter.

Many protists are well known for their capabilities of mixotrophy, that is, they can use chloroplasts to perform photosynthesis and feed and feed heterotrophically, for example, by ingestion of bacterioplankton through phagotrophy (Zubkov and Tarran, 2008; Stoecker *et al*., 2017; Terrado *et al*., 2017). Although occupying only a very small fraction of total phototrophic microbial eukaryote communities, investigations of 18S rRNA and psbA gene transcripts revealed the presence of Chrysophyceae-affiliated sequences in the deep Western Pacific Ocean (Figs 4C and 5A, Supporting Information Figs. S6 and S8). Chrysophytes are reported to be capable of phagotrophy, osmotrophy and phototrophy (Holen and Boraas 1995). Chrysophytes have been reported in the deep South China Sea (Xu *et al*., 2017b) and were identified as the second most abundant class in deep-sea protistan communities (Pernice *et al*., 2015b). Combined with their prevalence in the deep sea globally, it has been proposed that chrysophytes may be important bacterivores in deep waters (Pernice *et al*., 2015b). In addition to chrysophytes, haptophytes have been proposed to carry out most of the bacterivory in the surface layer of Atlantic Ocean (Zubkov and Tarran, 2008). In the present study, the NNN of some psbA sequences (i.e., 34 in total, 21 of which were recovered from ≥1000 m waters) is *Chrysochromulina* sp. (GenBank accession No. KJ201907, Supporting Information Table S2), a non-calcifying haptophyte belonging to Prymnesiales, some members of which are capable of mixotrophy (Kawachi *et al*., 1991; Tillmann, 1998; Legrand *et al*., 2001; Liu *et al*., 2009). Thus, it is possible that some of the phototrophic eukaryotic signals in the deep sea of the Western Pacific Ocean were from mixotrophs which thrive in the dark ocean by preying on other microbes. The global ubiquity of phototrophic microbial eukaryotes in deep oceanic waters and the contribution of mixotrophs to the total microbial eukaryote community needs further exploration in order to determine: (i) their contributions to the downward transportation of organic carbon and, (ii) the role of

mixotrophs in microbial food webs through predation in the dark ocean.

Experimental procedures

Sampling and environmental data collection

Samples for measuring microbial abundances (bacteria/archaea, *Prochlorococcus*, *Synechococcus*, pigmented picoeukaryotes and pigmented nano-sized eukaryotes) were collected at 12 depths (5, 25, 50, 75, 100, 200, 500, 1000, 1500, 2000, 2500 and 3000 m) within the epi- (0–200 m), meso- (200–1000 m) and bathy-pelagic (1000–4000 m) zones from 11 stations in the tropical Western Pacific Ocean (122–130° E, 1–23° N) from September 5 to October 3, 2015 aboard R/V Kexue (Fig. 1). At station P12, an additional sample was collected from 5000 m. Seawater was collected using Niskin bottles on a rosette containing a CTD profiler (Sea-Bird SBE 911plus), which determined water temperature and salinity. For the determination of bacteria/archaea, *Prochlorococcus*, *Synechococcus* and pigmented picoeukaryote (PPEs), five subsamples (2 ml each), pre-filtered using 20 μm mesh, were fixed with glutaraldehyde (final conc., 0.5%) at 4°C for 30 min and then stored at −80°C for later analysis after flash-freezing in liquid nitrogen. Depending on the depth, 50–250 ml of seawater was fixed with glutaraldehyde (final conc. 1%) at 4°C in the dark for 2 h before staining for the enumeration of pigmented nano-sized eukaryotes (PNEs). Two litres of seawater from certain stations and depths (3000 m at P6; 25 m, 75 m, 500 m and 3000 m at P8; 5000 m at P12; 25 m, 75 m and 3000 m at P14; 1000 m at P16) were pre-filtered using 200 μm Nitex (Sefar) to remove metazoans, and then filtered onto 47 mm diameter. Millipore ISOPORE membrane filters (0.45 μm pore size) to retain microbial eukaryotes. Filters were then immersed into RNA*later* solution (Ambion, CA, USA) and kept at −20°C until further processing for sequencing of 18S rRNA and psbA gene transcripts. Four to ten litres of seawater from each of three depths (5 m, DCM and 200 m) was filtered through a 47 mm GF/F glass fibre filter and immediately frozen in liquid nitrogen prior to phytoplankton pigment analysis in the laboratory. Samples were not available for pigment analysis at stations P8, P10 and P18 so seawater from stations P7 and P11 (not shown in Fig. 1), which were located mid-way between P6 and P8, and between P10 and P12, respectively, were used instead.

Abundance of prokaryotes, pigmented picoeukaryotes (PPEs) and pigmented nano-sized eukaryotes (PNEs)

The abundances of bacteria/archaea, *Prochlorococcus* and *Synechococcus*, and PPEs were analysed using a flow cytometer (Epics Altra II, Beckman Coulter) following procedures described previously (Marie *et al*., 1999; Jiao *et al*., 2014). The abundance of PNEs was determined by examining stained cells by epifluorescence microscopy at 1000× magnification (Nikon Optiphot-2). Cells of PNEs were stained with 4′6-diamidino-2-phenylindole (DAPI, final conc., 0.1 μg ml^{-1}) and collected on 0.8 μm pore-size dark Nuclepore filters (Millipore) under low pressure (< 100 mmHg) (Porter and Feig, 1980; Not *et al*., 2008). PNEs were identified by their red fluorescence under blue excitation light. To obtain reliable estimates of their abundance, at least 50 cells were counted. PNEs were further classified into three size classes (2–5, 5–10 and 10–20 μm) using an ocular micrometre.

Phytoplankton pigment composition

Phytoplankton composition was inferred using pigment markers as indicators. Chl *a*, an indicator for total phytoplankton biomass, referred to the sum of monovinyl and divinyl Chl *a.* Pigment analysis followed the protocol according to Huang and colleagues (2010). Briefly, phytoplankton pigments were extracted in N,N-dimethylformamide (Furuya and Marumo, 1983) and analyzed using High Performance Liquid Chromatography (Agilent Series 1100, Agilent Technologies) system fitted with a 3.5-mm Eclipse XDB C8 column (100 × 4.6 mm; Agilent Technologies) following a modification of the method of Mantoura and Llewellyn (1983) and Van Heukelem and Thomas (2001). Based on pigment data, the phytoplankton community was determined using CHEMTAX software (Mackey *et al*., 1996).

RNA extraction, PCR amplification, high-throughput sequencing and processing of the hyper-variable V9 regions of the 18S rRNA

Total RNA was extracted from each cryopreserved filter membrane using AllPrep DNA/RNA kit (Qiagen, USA) following the protocols of Sun and colleagues (2017) and Xu and colleagues (2017b). Extracted RNA was quantified using a Nanodrop ND-2000 Spectrophotometer (Labtech International, USA) and the integrity was assessed by 1.5% agarose gel electrophoresis. After treatment with DNase (Qiagen, Germany) to remove the carry-over genomic DNA, RNA was reverse-transcribed into cDNA using QuantiTect® Reverse Transcription kit (Qiagen, USA). Genomic DNA was further removed by gDNA Wipeout Buffer supplied within the kit. The hypervariable loop V9 regions of the 18S rRNA were amplified by applying the universal primers, 1389F and 1510R (Amaral-Zettler *et al*., 2009). Five individual PCR reactions for each sample were run and pooled to minimize reaction-level PCR bias (Bates *et al*., 2013) and to collect

sufficient amplicons for sequencing. The resulting PCR amplicons (ca. 130 bp) were excised from the gel using MiniElute Gel Extraction Kit (Qiagen, USA). All purified amplicons were sent to a commercial company for paired-end sequencing with Illumina MiSeq platform. Sequences generated were deposited in NCBI Sequence Read Archive (accession number SRP159133).

Quality filtering, demultiplexing and assembly of raw data were performed following Li and colleagues (2018) using Trimmomatic and Flash software (Magoc and Salzberg, 2011; Bolger *et al*., 2014). Chimeras were identified and removed with UCHIME (Edgar *et al*., 2011) using both *de novo* and reference-based chimera searches against the PR2 database (De Vargas *et al*., 2015). Singletons were further removed and reads were clustered into Operational Taxonomic Units (OTUs) at 95% sequence similarity using UPARSE (Edgar, 2013). Generation of OTU tables and taxonomic assignment of OTUs were done with QIIME by UCLUST against the PR2 database (Caporaso *et al*., 2010). OTUs that were affiliated with Bacteria or Archaea, plastidial sequences, those assigned as Metazoa and those 'Unassigned' were discarded. To normalize sampling effort, sequences were normalized by randomly resampling 7078 reads per sample (the lowest number of sequences recovered for all samples). Alpha diversity estimators (Chao1, Shannon, ACE, Inverse of Simpson and Phylogenetic Diversity) were calculated using QIIME (Caporaso *et al*., 2010). To assess similarities between communities, pairwise similarities among samples were calculated by Bray–Curtis similarity coefficient (Legendre and Legendre, 1998). Similarity matrices were visualized using Non-Metric Multidimensional Scaling (nMDS) diagrams. The differences among groupings from cluster analysis were tested by ANOSIM. To check the robustness of dissimilarity among communities, beta diversity was calculated using the unweighted Unifrac metric (Lozupone and Knight, 2005) and community dissimilarity was shown using a two-dimensional principal coordinate analysis (PCoA).

Amplification, cloning, sequencing and processing of psbA gene transcripts

PsbA gene fragments (ca., 750 bp) were amplified from reverse-transcribed cDNA using primers psbA-1F and psbA-2R designed by Wang and Chen (2008). For each sample, PCR products from five separate reactions were pooled and clone libraries were constructed using TA cloning kit (TaKaRa, China) according to the manufacturer's instructions. Between 120 and 200 positive clones from each sample were commercially sequenced using M13F and M13R primers from both ends using an ABI 3730xl DNA Analyzer.

The obtained psbA sequences were automatically assembled and then manually checked using Sequencher 5.0 (Gene-Codes Corp., MI, USA). Each sequence was blasted against the GenBank database and sequences of prokaryote or virus/phage origin were excluded from the analysis. Potential chimeric sequences were detected using UCHIME (Edgar *et al*., 2011) using the *de novo* method and then removed. An OTU table was constructed by clustering sequences to OTUs at a 99% similarity threshold using UPARSE (Edgar, 2013). The most abundant sequence within each OTU was selected as the OTU representative sequence. OTUs were then taxonomically assigned by BLAST search against nr-NCBI and the nearest neighbour (NN) and the nearest named neighbour (NNN) were identified (Scheckenbach *et al*., 2010; Xu *et al*., 2017a). All environmental psbA sequences generated in this study were deposited in GenBank under accession numbers MH881756 - MH882415.

Acknowledgements

We thank the captain, crew and marine technicians of the R/V Kexue during the cruise (NORC-2015) for ensuring smooth sampling. This work was supported by the National Key Research Programs (2016YFA0601400) and the National Natural Science Foundation of China (NSFC) (91751207, 41876142 and 31772426). Special thanks are given to two anonymous reviewers for their valuable comments. The authors declare no conflict of interest.

References

Agusti, S., González-Gordillo, J. I., Vaqué, D., Estrada, M., Cerezo, M. I., Salazar, G., *et al*. (2015) Ubiquitous healthy diatoms in the deep sea confirm deep carbon injection by the biological pump. *Nat Commun* **6**: 7608.

Amaral-Zettler, L. A., McCliment, E. A., Ducklow, H. W., and Huse, S. M. (2009) A method for studying protistan diversity using massively parallel sequencing of V9 hypervariable regions of small-subunit ribosomal RNA genes. *PLoS One* **4**: e6372.

Bates, S. T., Clemente, J. C., Flores, G. E., Walters, W. A., Parfrey, L. W., Knight, R., and Fierer, N. (2013) Global biogeography of highly diverse protistan communities in soil. *ISME J* **7**: 652–659.

Bienfang, P. K. (1980) Phytoplankton sinking rates in oligotrophic waters off Hawaii, USA. *Mar Biol* **61**: 69–77.

Bolger, A. M., Lohse, M., and Usadel, B. (2014) Trimmomatic: a flexible trimmer for Illumina sequence data. *Bioinformatics* **30**: 2114–2120.

Caporaso, J. G., Kuczynski, J., Stombaugh, J., Bittinger, K., Bushman, F. D., Costello, E. K., *et al*. (2010) QIIME allows analysis of high-throughput community sequencing data. *Nat Methods* **7**: 335–336.

Cadée, G. C. (1985) Macroaggregates of *Emiliana huxleyi* in sediment traps. *Mar Ecol Prog Ser* **24**: 193–196.

Decelle, J., Romac, S., Stern, R. F., Bendif, E. M., Zingone, A., Audic, S., *et al*. (2015) PhytoREF: a reference database of the plastidial 16S rRNA gene of photosynthetic eukaryotes with curated taxonomy. *Mol Ecol Resour* **15**: 1435–1445.

De Vargas, C., Audic, S., Henry, N., Decelle, J., Mahé, F., Logares, R., *et al*. (2015) Eukaryotic plankton diversity in the sunlit ocean. *Science* **348**: 1261605.

Edgar, R. C. (2013) UPARSE: highly accurate OTU sequences from microbial amplicon reads. *Nat Methods* **10**: 996–998.

Edgar, R. C., Haas, B. J., Clemente, J. C., Quince, C., and Knight, R. (2011) UCHIME improves sensitivity and speed of chimera detection. *Bioinformatics* **27**: 2194–2200.

Falkowski, P. G., Katz, M. E., Knoll, A. H., Quigg, A., Raven, J. A., Schofield, O., and Taylor, F. J. R. (2004) The evolution of modern eukaryotic phytoplankton. *Science* **305**: 354–360.

Field, C. B., Behrenfeld, M. J., Randerson, J. T., and Falkowski, P. (1998) Primary production of the biosphere: integrating terrestrial and oceanic components. *Science* **281**: 237–240.

Furuya, K., and Marumo, R. (1983) The structure of the phytoplankton community in the subsurface chlorophyll maxima in the western North Pacific Ocean. *J Plankton Res* **5**: 393–406.

Holen, D. A., and Boraas, M. E. (1995)Mixotrophy in chrysophytes . In *Chrysophyte Algae Ecology, Phylogeny and Development*, Sandgren, C. D., Smol, J. P., and Kristiansen, J. (eds). Leiden: Cambridge University Press, pp. 119–140.

Huang, B., Hu, J., Xu, H., Cao, Z., and Wang, D. (2010) Phytoplankton community at warm eddies in the northern South China Sea in winter 2003/2004. *Deep-Sea Res Part II* **57**: 1792–1798.

Iversen, M. H., and Ploug, H. (2010) Ballast minerals and the sinking carbon flux in the ocean: carbon-specific respiration rates and sinking velocities of marine snow aggregates. *Biogeosciences* **7**: 2613–2624.

Jardillier, L., Zubkov, M. V., Pearman, J., and Scanlan, D. J. (2010) Significant CO_2 fixation by small prymnesiophytes in the subtropical and tropical Northeast Atlantic Ocean. *ISME J* **4**: 1180–1192.

Jiao, N., Luo, T., Zhang, R., Yan, W., Lin, Y., Johnson, Z. I., *et al*. (2014) Presence of *Prochlorococcus* in the aphotic waters of the western Pacific Ocean. *Biogeosciences* **11**: 2391–2400.

Karl, D. M., Church, M. J., Dore, J. E., Letelier, R. M., and Mahaffey, C. (2012) Predictable and efficient carbon sequestration in the North Pacific Ocean supported by symbiotic nitrogen fixation. *Proc Natl Acad Sci USA* **109**: 1842–1849.

Kawachi, M., Inouye, I., Maeda, O., and Chihara, M. (1991) The haptonema as a food-capturing device: observations on *Chrysochromulina hirta* (Prymnesiophyceae). *Phycologia* **30**: 63–573.

Kimball, J., Corcoran, E. F., and Wood, F. E. (1963) Chlorophyll-containing microorganisms in the aphotic zone of the oceans. *Bull Mar Sci* **13**: 574–577.

Komar, P. D., Morse, A. P., Small, L. F., and Fowler, S. W. (1981) An analysis of sinking rates of natural copepod and euphausiid fecal pellets. *Limnol Oceanogr* **26**: 172–180.

Lampitt, R. S., Wishner, K. E., Turley, C. M., and Angel, M. V. (1993) Marine snow studies in the Northeast Atlantic Ocean: distribution, composition and role as a food source for migrating plankton. *Mar Biol* **116**: 689–702.

Legendre, P., and Legendre, L. (1998) Numerical Ecology. Elsevier: The Netherlands, Amsterdam.

Legrand, C., Johansson, N., Johnsen, G., Børsheim, K. Y., and Granéli, E. (2001) Phagotrophy and toxicity variation in the mixotrophic *Prymnesium patelliferum* (Haptophyceae). *Limnol Oceanogr* **46**: 1208–1214.

Li, W. K. W. (1995) Composition of ultraphytoplankton in the Central North Atlantic. *Mar Ecol Prog Ser* **122**: 1–8.

Li, W. K. W. (2009) From cytometry to macroecology: a quarter century quest in microbial oceanography. *Aquat Microb Ecol* **57**: 239–251.

Li, R., Jiao, N., Warren, A., and Xu, D. (2018) Changes in community structure of active protistan assemblages from the lower Pearl River to coastal waters of the South China Sea. *Eur J Protistol* **63**: 72–82.

Liu, H., Probert, I., Uitz, H., Claustre, H., Aris-Brosou, S., Frada, M., *et al*. (2009) Extreme diversity in noncalcifying haptophytes explains a major pigment prardox in open oceans. *Proc Natl Acad Sci USA* **106**: 12803–12808.

Lovejoy, C., Massana, R., and Pedros-Alio, C. (2006) Diversity and distribution of marine microbial eukaryotes in the Arctic Ocean and adjacent seas. *Appl Environ Microbiol* **72**: 3085–3095.

Lozupone, C., and Knight, R. (2005) UniFrac: a new phylogenetic method for comparing microbial communities. *Appl Environ Microbiol* **71**: 8228–8235.

Mackey, M. D., Mackey, D. J., Higgins, H. W., and Wright, S. W. (1996) CHEMTAX-a program for estimating class abundances from chemical markers: application to HPLC measurements of phytoplankton. *Mar Ecol Prog Ser* **144**: 265–283.

Magoc, T., and Salzberg, S. L. (2011) FLASH: fast length adjustment of short reads to improve genome assemblies. *Bioinformatics* **27**: 2957–2963.

Man-Aharonovich, D., Philosof, A., Kirkup, B. C., Gall, F. L., Yogev, T., Berman-Frank, I., *et al*. (2010) Diversity of active marine picoeukaryotes in the eastern Mediterranean Sea unveiled using photosystem-II *psbA* transcripts. *ISME J* **4**: 1044–1052.

Mantoura, R. F. C., and Llewellyn, C. A. (1983) The rapid determination of algal chlorophyll and carotenoid pigments and their break down products in natural waters by reverse phase high performance liquid chromatography. *Anal Chim Acta* **121**: 297–314.

Marañón, E., Holligan, P. M., Barciela, R., González, N., Mouriño, B., Pazó, M. J., and Varela, M. (2001) Patterns of phytoplankton size structure and productivity in contrasting open-ocean environments. *Mar Ecol Prog Ser* **216**: 43–56.

Marie, D., Partensky, F., Vaulot, D., and Brussaard, C. (1999) Enumeration of phytoplankton, bacteria, and viruses in marine samples. *Curr Protoc Cytom* **11**: 1–15.

Massana, R. (2011) Eukaryotic picoplankton in surface oceans. *Annu Rev Microbiol* **65**: 91–110.

Massana, R., Balagué, V., Guillou, L., and Pedrós-Alió, C. (2004a) Picoeukaryotic diversity in an oligotrophic coastal site studied by molecular and culturing approaches. *FEMS Microbiol Ecol* **50**: 231–243.

Massana, R., Castresana, J., Balagué, V., Guillou, L., Romari, K., Groisillier, A., *et al*. (2004b) Phylogenetic and ecological analysis of novel marine stramenopiles. *Appl Environ Microbiol* **70**: 3528–3534.

Moon-van der Staay, S. Y., De Wachter, R., and Vaulot, D. (2001) Oceanic 18S rDNA sequences from picoplankton reveal unsuspected eukaryotic diversity. *Nature* **409**: 607–610.

Nagata, T., Tamburini, C., Arístegui, J., Baltar, F., Bochdansky, A. B., Fonda-Umani, S., *et al*. (2010) Emerging concepts on microbial processes in the bathypelagic ocean – ecology, biogeochemistry, and genomics. *Deep Sea Res Part II* **57**: 1519–1536.

Not, F., Latasa, M., Scharek, R., Viprey, M., Karleskind, P., Balagué, V., *et al*. (2008) Protistan assemblages across the Indian Ocean, with a specific emphasis on the picoeukaryotes. *Deep Sea Res Part I* **55**: 1456–1473.

Pernice, M. C., Forn, I., Gomes, A., Lara, E., Alonso-Sáez, L., Arrieta, J. M., *et al*. (2015a) Global abundance of planktonic heterotrophic protists in the deep ocean. *ISME J* **9**: 782–792.

Pernice, M. C., Giner, C. R., Logares, R., Perera-Bel, J., Acinas, S. G., Duarte, C. M., *et al*. (2015b) Large variability of bathypelagic microbial eukaryotic communities across the world's oceans. *ISME J* **10**: 945–958.

Ploug, H., Iversen, M., Koski, M., and Buitenhuis, E. T. (2008) Production, oxygen respiration rates, and sinking velocity of copepod fecal pellets: direct measurements of ballasting by opal and calcite. *Limnol Oceanogr* **53**: 469–476.

Porter, K. G., and Feig, Y. S. (1980) The use of DAPI for identifying and counting aquatic microflora. *Limnol Oceanogr* **25**: 943–948.

Richardson, T. L., and Jackson, G. A. (2007) Small phytoplankton and carbon export from the surface ocean. *Science* **315**: 838–840.

Scharek, R., Tupas, L. M., and Karl, D. M. (1999) Diatom fluxes to the deep sea in the oligotrophic North Pacific gyre at station ALOHA. *Mar Ecol Prog Ser* **182**: 55–67.

Scheckenbach, F., Hausmann, K., Wylezich, C., Weitere, M., and Arndt, H. (2010) Large-scale patterns in biodiversity of microbial eukaryotes from the abyssal sea floor. *Proc Natl Acad Sci USA* **107**: 115–120.

Schlitzer, R.*Ocean Data View*. 2010. Bremerhaven, Germany. Alfred Wegener Institute. URL http://odv.awi.de.

Sigman, D. M., and Haug, G. H. (2006)The biological pump in the past . In *Treatise on Geochemistry*, Holland, H. D., and Turekian, K. K. (eds). Oxford: Pergamon Press, pp. 491–528.

Simon, M., Grossart, H. P., Schweitzer, B., and Ploug, H. (2002) Microbial ecology of organic aggregates in aquatic ecosystems. *Aquat Microb Ecol* **28**: 175–211.

Smayda, T. J. (1971) Normal and accelerated sinking of phytoplankton in the sea. *Mar Geol* **11**: 105–122.

Stoecker, D. K., Hansen, P. J., Caron, D. A., and Mitra, A. (2017) Mixotrophy in the marine plankton. *Annu Rev Mar Sci* **9**: 311–335.

Sun, P., Huang, L., Xu, D., Huang, B., Chen, N., and Warren, A. (2017) Marked seasonality and high spatial variation in estuarine ciliates are driven by exchanges between the 'abundant' and 'intermediate' biospheres. *Sci Rep* **7**: 9494.

Terrado, R., Pasulka, A. L., Lie, A. A., Orphan, V. J., Heidelberg, K. B., and Caron, D. (2017) Autotrophic and heterotrophic acquisition of carbon and nitrogen by a mixotrophic chrysophyte established through stable isotope analysis. *ISME J* **11**: 2022–2034.

Tillmann, U. (1998) Phagotrophy of a plastidic haptophyte, *Prymnesium patelliferum*. *Aquat Microb Ecol* **14**: 155–160.

Van Heukelem, L., and Thomas, C. S. (2001) Computer-assisted high-performance liquid chromatography method development with applications to the isolation and analysis of phytoplankton pigments. *J Chromatogr* **10**: 31–49.

Vaulot, D., Romari, K., and Not, F. (2002) Are autotrophs less diverse than heterotrophs in marine picoplankton? *Trends Microbiol* **10**: 266–267.

Wang, K., and Chen, F. (2008) Prevalence of highly host specific cyanophages in the estuarine environment. *Environ Microbiol* **10**: 300–312.

Wiebe, P. H., Remsen, C. C., and Vaccaro, R. F. (1974) *Halosphaera viridis* in the Mediterranean Sea: size range, vertical distribution, and potential energy source for deep-sea benthos. *Deep Sea Res Oceanogr Abstr* **21**: 657–667.

Worden, A. Z., Nolan, J. K., and Palenik, B. (2004) Assessing the dynamics and ecology of marine picophytoplankton: the importance of the eukaryotic component. *Limnol Oceanogr* **49**: 168–179.

Xu, D., Jiao, N., Ren, R., and Warren, A. (2017a) Distribution and diversity of microbial eukaryotes in bathypelagic waters of the South China Sea. *J Eukaryot Microbiol* **64**: 370–382.

Xu, D., Li, R., Hu, C., Sun, P., Jiao, N., and Warren, A. (2017b) Microbial eukaryote diversity and activity in the water column of the South China Sea based on DNA and RNA high throughput sequencing. *Front Microbiol* **8**: 1121.

Yang, G., Wang, F., Li, Y., and Lin, P. (2013) Mesoscale eddies in the northwestern subtropical Pacific Ocean: statistical characteristics and three-dimensional structures. *J Geophys Res-Oceans* **118**: 1906–1925.

Yuan, D., Han, W., and Hu, D. (2007) Anti-cyclonic eddies northwest of Luzon in summer-fall observed by satellite altimeters. *Geophys Res Lett* **34**: L13610.

Zeidner, G., and Béjà, O. (2004) The use of DGGE analyses to explore eastern Mediterranean and Red Sea marine picophytoplankton assemblages. *Environ Microbiol* **6**: 528–534.

Zeidner, G., Preston, C. M., Delong, E. F., Massana, R., Post, A. F., Scanlan, D. J., and Béjà, O. (2003) Molecular diversity among marine picophytoplankton as revealed by psbA analyses. *Environ Microbiol* **5**: 212–216.

Zubkov, M. V., and Tarran, G. A. (2008) High bacterivory by the smallest phytoplankton in the North Atlantic Ocean. *Nature* **455**: 224–226.

Supporting Information

Additional Supporting Information may be found in the online version of this article at the publisher's web-site:

Fig S1. Distribution of environmental parameters in the water column of the Western Pacific Ocean. (A) Temperature, (B) Salinity, (C) Chlorophyll *a.* The map was generated using Ocean Data View 4 software (Schlitzer,).

Fig. S2. Relative contribution of six eukaryotic phytoplankton groups to total eukaryotic phytoplankton Chl *a*, as distinguished by their pigment suites after CHEMTAX analysis at 5 m (A), DCM (B), 200 m (C), respectively, and absolute Chl *a* concentration attributed to haptophytes (D).

Fig. S3. Distribution of picoplankton abundance in the Western Pacific Ocean. A. Bacteria/archaea ($\times 10^5$ cells mL^{-1}). B. *Synechococcus* ($\times 10^3$ cells mL^{-1}). C. *Prochlorococcus* ($\times 10^5$ cells mL^{-1}). D. Pigmented picoeukaryotes ($\times 10^3$ cells mL^{-1}). The map was generated using Ocean Data View software (Schlitzer, 2010).

Fig. S4. Pigmented nano-sized eukaryotes (PNEs) as seen by epifluorescence microscopy after DAPI staining. Same cell under UV excitation for DAPI-stained DNA blue fluorescence (A) and under blue excitation for Chl *a* red fluorescence (B) respectively. PNEs under blue excitation for Chl *a* red fluorescence, showing different cell shapes (C-F). Scale bars = 5 μm.

Fig. S5. Relative sequence abundance (A) and OTU richness (B) of microbial eukaryotes in the Western Pacific Ocean at the supergroup taxonomic level comparing shallow (25 and 75 m) and deep (≥ 500 m) waters as revealed by sequencing of the V9 regions of 18S rRNA.

Fig. S6. Community composition of microbial eukaryotes at the supergroup taxonomic level in each sample revealed by sequencing of the V9 regions of 18S rRNA.

Fig. S7. The top 10 dominant groups in each deep-sea sample. Note that phototrophic groups contributed substantially in each sample.

Fig. S8. Relative psbA sequence abundance of phototrophic microbial eukaryotes in the water column of the Western Pacific Ocean.

Table S1. Diversity estimates of Western Pacific Ocean samples. $OTU_{0.05}$: Operational taxonomic unit at 95% 18S rRNA V9 region gene sequence identity. * reads affiliated with microbial eukaryotes only; ** Standardized numbers based on subsampling of 7708 sequences without replacement.

Table S2. All psbA OTUs with their Nearest Named Neighbour, genetic distance and species names in the GenBank database.